Identification of the proteins determining the blood circulation time of nanoparticles

Marques, Cintia; Hajipour, Mohammad Javad; Marets, Célia; Oudot, Alexandra; Safavi-sohi, Reihaneh; Guillemin, Mélanie; Borchard, Gerrit; Jordan, Olivier; Saviot, Lucien; Maurizi, Lionel

How to cite

MARQUES, Cintia et al. Identification of the proteins determining the blood circulation time of nanoparticles. In: ACS nano, 2023, vol. 17, n° 13, p. 12458–12470. doi: 10.1021/acsnano.3c02041

This publication URL: https://archive-ouverte.unige.ch/unige:184307
Publication DOI: 10.1021/acsnano.3c02041

Identification of the Proteins Determining the Blood Circulation Time of Nanoparticles

Cintia Marques[1,2†*], Mohammad Javad Hajipour[3†*], Célia Marets[4], Alexandra Oudot[5], Reihaneh Safavi-Sohi[6], Mélanie Guillemin[5] Gerrit Borchard[1,2], Olivier Jordan[1,2], Lucien Saviot[4], Lionel Maurizi[4*]

[1] Institute of Pharmaceutical Sciences of Western Switzerland, University of Geneva, 1 Rue Michel Servet, 1211 Geneva, Switzerland;

[2] Section of Pharmaceutical Sciences, University of Geneva, 1 Rue Michel Servet, 1211 Geneva;

[3] Department of Radiology, Molecular Imaging Program at Stanford (MIPS), Stanford University, Stanford, California, USA

[4] Laboratoire Interdisciplinaire Carnot de Bourgogne (ICB), UMR 6303 CNRS – Université de Bourgogne Franche-Comté, BP 47870, Dijon Cedex, F-21078, France.

[5] Plateforme d'Imagerie Préclinique, Service de Médecine Nucléaire, Centre Georges François Leclerc, 21000 Dijon, France

[6] Department of Chemistry and Biochemistry, University of Notre Dame, Indiana, USA

† These authors contributed equally to this work

* Correspondence: cintia.baptistamarques@unige.ch, hajipour@stanford.edu, lionelmaurizi@gmail.com

ABSTRACT

The therapeutic efficacy and adverse impacts of nanoparticles (NPs) are strongly dependent on their systemic circulation time. The corona proteins adsorbed on the NPs determine their plasma half-lives and hence, it is crucial to identify the proteins shortening or extending their circulation time. In this work, the *in vivo* circulation time and corona composition of superparamagnetic iron oxide nanoparticles (SPIONs), with different surface charges/chemistries, over time. SPIONs with neutral and positive charges showed the longest and shortest circulation times, respectively. The most striking observation was that corona-coated NPs with similar opsonin/dysopsonin content showed different circulation times implying these biomolecules are not the only contributing factors. Long-circulating NPs adsorb higher concentrations of osteopontin, lipoprotein lipase, coagulation factor VII, matrix Gla protein, secreted phosphoprotein 24, alpha-2H-glycoprotein, and apolipoprotein C-I, while short-circulating NPs adsorb higher amounts of hemoglobin. Therefore, these proteins may be considered determining factors governing the NP systemic circulation time.

Keywords: nanoparticle, protein corona, blood circulation time, opsonin, dysopsonin

INTRODUCTION

Nanotechnology has the potential to revolutionize medicine and overcome the challenges associated with the current therapeutic and diagnostic approaches [1-5]. Thanks to their small size, high surface-to-volume ratio, ease of synthesis and modification, and capability to pass through biological barriers, NPs are considered candidates for the delivery of drugs or contrast agents to cells/tissues of interest in the animal/human body [4]. However, the application of NPs in medicine is often challenged by the biomolecular corona [6]. NPs surfaces are immediately covered by layers of biomolecules called the biomolecular/protein corona when they enter the human/animal body and are exposed to biological media (*e.g.,* blood, lymphatic fluid)[7-10]. The biomolecules adsorbed onto the NPs change their physicochemical properties and give them a new biological identity that is different from their synthetic identity[11-13]. Depending on the individual corona composition and its composition, the corona-coated NPs show different behavior [14-17]. For example, the biomolecular corona may affect the pharmacokinetics of NPs such as plasma half-life and distribution [18]. Among the biomolecules adsorbed on NPs, opsonins, such as complement factors and/or immunoglobulins (IgG), mediate NP binding to macrophages and phagocytes and therefore, NP clearance is increased. Albumin, Histidine Rich Glycoprotein, Clusterin, Apo J, Apo A4, Apo C3 on the contrary, prolong the blood circulation time of NPs, acting as a dysopsonin [19-21]. Therefore, the retention time of NPs in blood circulation is dependent on the proteins adsorbed onto their surfaces [22]. To improve the diagnostic and therapeutic efficacy of NPs, their retention time in blood circulation is of great importance. NPs with longer blood circulation times have a higher probability to be accumulated in cells/tissues of interest, but to do so, NPs must escape from phagocytes of the reticuloendothelial

system (RES). Strategies to escape immune recognition and prolong NP circulation time include allowing NPs to hitchhike on cell membrane, NP coating with a cell membrane cloak, and NP coating with poly(ethylene glycol) (PEG), polysaccharides, zwitterionic structures or other hydrophilic polymers [23-26]. NPs coating with the mentioned polymers successfully reduces protein adsorption, however, the biomolecular corona can still be detected [27]. Since corona decoration determines NP blood circulation half-life [22], it is crucial to better understand which proteins could bind NPs to modulate clearance/retention time under *in vivo* conditions. The opsonins/dysopsonins, which have been introduced as key determinants of NP circulation time, are dominantly adsorbed onto the surface of NPs. However, NPs show different circulation times in the animal body. Based on this evidence, we hypothesized there should be some proteins that could strongly govern the NP retention time and have not yet been recognized. To check this hypothesis, SPIONs were coated with polyvinyl alcohol (PVA) of different molecular weights (12 and 31 kDa) exhibiting different terminal groups at their surface either hydroxyl (OH), carboxyl (COOH) or amino (NH_2) end groups. The different functional groups yielded NPs with, respectively, neutral ([0]), negative (-) and positive (+) charges. We tracked the NP circulation times and their corona compositions over time upon intravenous (i.v.) injection in rats. Reproducibility and repeatability of the experiments were assessed and, using this strategy, we identified proteins that may be involved in the modulation of blood circulation time of NPs.

RESULTS AND DISCUSSION

NP synthesis and characterization

SPIONs with an average diameter of 8 nm were synthesized by co-precipitation (Table 1 and Figure S1-a). The hydrodynamic diameter of naked SPIONs was around 70 nm in intensity proving that the elemental crystallites aggregated during the synthesis process into small packed NPs as seen in Table 1 and Figure S1-a. Naked SPIONs are also neutral in physiological conditions.

SPIONs were coated with 12 and 31 kDa PVA to prepare SPIONs-PVA with different polymer packing and charges due to the different molecular weights of PVA (Table S1). After coating with PVA, the NP hydrodynamic size increased to more than 100 nm and SPIONs are still a little bit aggregated into small NPs packs as seen on the TEM picture in Figures S1-b and c. PVA, which is commonly applied as a surfactant, is known to adsorb nonspecifically onto SPIONs through hydrogen interactions. Thus, polymer adsorption onto the SPIONs core is not only a result of SPIONs-PVA interaction but also PVA-PVA interaction, leading to similar sizes of PVA coated-SPIONs (12 kDa vs 31 kDa). This behavior differs from other polymers, such as PEG, which tends to form brush-like structures, resulting in a more direct MW-size dependency. Thus, despite the SPIONs-PVA charges being tuned with the different chosen PVA, their hydrodynamic diameters were not influenced by the molecular weights of PVA. Size is an essential factor in the development of long-circulating NPs. NPs with a size of less than 10 nm are rapidly cleared from blood circulation by renal excretion. Larger NPs, which avoid renal excretion, are mainly removed by opsonization. For example, NPs with a size of 240 nm are cleared faster than those with a size of 60 or 80 nm [28, 29]. Therefore, the size of long-circulating NPs should be between 10-200 nm to be small enough to escape from opsonization and RES

uptake and large enough to not be removed by renal filtration. Based on this assumption, the synthesized SPIONs-PVA appear to fit for the purpose of studying NP circulation time.

NP surface modification with different types of polymers (polysaccharides and PEG) is an efficient strategy to reduce the NP hydrophobicity and charge density, both of which are triggers of opsonization [29]. In some cases, however, the polymers prevent opsonization while activating the complement system. Therefore, the type of polymer used for surface coating and surface charge should be carefully considered. The physicochemical properties (size, charge, and Polydispersity Index (PDI)) of NPs used in this study are listed in Table 1 and Table S2). The adsorption of proteins on the NPs surfaces increased their size and PDI. As shown in Table S2, FBS has a high PDI around 0.447, due to the different proteins that can be found and potential protein aggregation. After incubation, the FBS polydispersity contributes to the increase of the PDI compared to the NPs alone. Proteins also changed the zeta potentials of SPIONs-PVA to negative values. Statistically, positively charged SPIONs-PVA have a lower zeta potential than the neutral ones, which also have a lower zeta potential than the negatively charged NPs. Figure S2 shows the DLS measurements, from which we can conclude that FBS incubation did not lead to NPs aggregation.

Table 1. Physicochemical properties of SPIONs coated with PVA of different molecular weights and functional groups, in NaCl 0.15M at pH 7.4 (pH3 for naked SPIONs). Diameter obtained by TEM (dTEM); Hydrodynamic diameter (dH).

Naked SPIONs physicochemical characterizations					
NP name	**pH**	**DTEM (nm)**	**dH intensity (nm)**	**Zeta potential at pH 7.4 (mV)**	**PDI**
Naked	3	8	71	+2 ± 2	0.142 ± 0.007

SPIONs-PVA			Physicochemical properties		
NP name	Functional group	Molecular weight (kDa)	dH intensity (nm)	Zeta potential (mv)	PDI
12 +	NH_2	12	156	+5 ± 1	0.191 ± 0.017
12 [0]	OH		124	0 ± 1	0.171 ± 0.053
12-	COOH		144	-4 ± 1	0.156 ± 0.024
31 +	NH_2	31	147	+6 ± 1	0.159 ± 0.018
31 [0]	OH		126	0 ± 1	0.134 ± 0.007
31 -	COOH		146	-3 ± 1	0.142 ± 0.015

NP circulation time

To determine the systemic circulation time of SPIONs-PVA with different molecular weights and surface chemistry, the NPs were administered to rats by tail-vein injection and then blood samples were collected at different times (5, 10, 20, 30, 45, 60, 90 or 120 and 120 or 240 min) depending on the SPIONs concentrations over time (more details of protocols in SI). As different routes of injection can affect the blood circulation time, biodistribution, and corona decoration, all the NPs were injected by tail vein and in a similar manner.

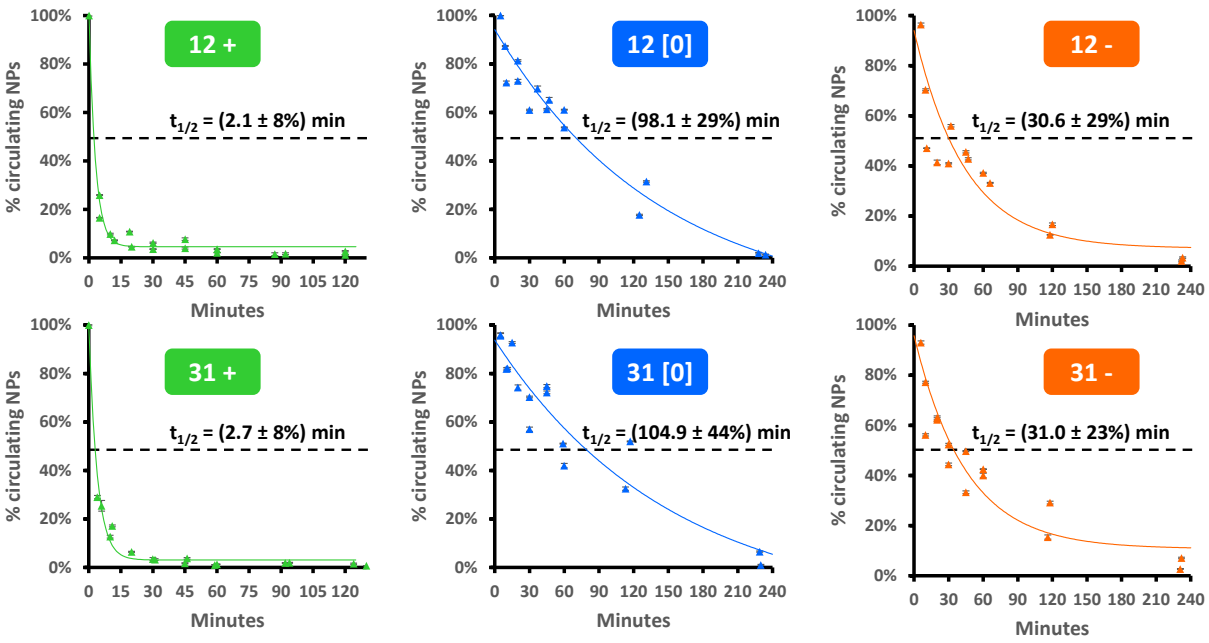

Figure 1. Systemic circulation time of the different SPIONs-PVA injected in rat blood stream. The half-lives and their standard deviation (given as percentage of the mean values) were obtained by fitting the points taking into account their uncertainties (duplicate experiments, triplicate analyses).

The data obtained from this analysis (Figure 1) showed that SPIONs-OH (neutral charge) had the longest circulation time with 90 minutes half-life. SPIONs-NH_2 (positive charge) had the shortest circulation time and were cleared after 15 min. SPIONs-COOH (negative charge) plasma half-life is 30 min. Studies suggest that NPs over 100 nm are mainly eliminated by the liver, spleen, and mesenteric lymph nodes [30, 31]. In accordance with this, our previous study has shown that, after 15 min, positive SPIONs-PVA are mainly found in the liver, while negative and neutral NPs are found in the serum[32]. In addition, the percentage of PVA-coated SPIONs found in the spleen was low, suggesting that these NPs are mainly eliminated through hepatic clearance. Tsoi et al.,[30] demonstrated that hepatic clearance of NPs over 100 nm happens due to Kupffer cells and B cells phagocytosis in the liver, which was correlated with ligands density on the NP (such as corona proteins), and not necessarily with NP surface chemistry. The desired surface chemistries and charges reported for extending the NP retention time in blood circulation, and/or preventing rapid NP clearance or accumulation in off-target organs are different for various NPs. For example, neutral and negatively charged PEG-PDLLA micelles showed similar circulation times while neutral and positively charged liposomes had a longer retention time compared to negatively charged ones [33, 34]. The researchers believe that contradictions in available reports might be related to the differences in composition, physicochemical properties, and surface chemistry of NPs. Any change in NP properties can affect the biomolecule adsorption on the NPs and consequent corona composition and content. According to our hypothesis, differences in NP

systemic circulation time might be related to differences in corona decorations on their surfaces. SPIONs-PVAs showed different circulation times which seems to be dependent on their surface charge/functional group (Figure 1) but not on the PVA's MV. The zeta potential values of all NPs were almost similar (-3.9 to -7.5) after the formation of protein corona on their surfaces (Table 1 and Table S2). This implies that the retention time of NPs in the blood circulation system is governed by the protein corona decoration dictated by the NP surface charge/functional group.

Therefore, we identified the proteins adsorbed onto the NPs at different time points. After tail vein injection of NPs, the blood samples were collected at different time points, centrifuged and then the obtained plasma fractions were passed through a hollow magnetic device to isolate NPs/proteins complexes. At the final step, the biomolecules adsorbed onto the NPs were identified by LC-ESI-MS/MS (Figure 2 and Figure S3, n = 3).

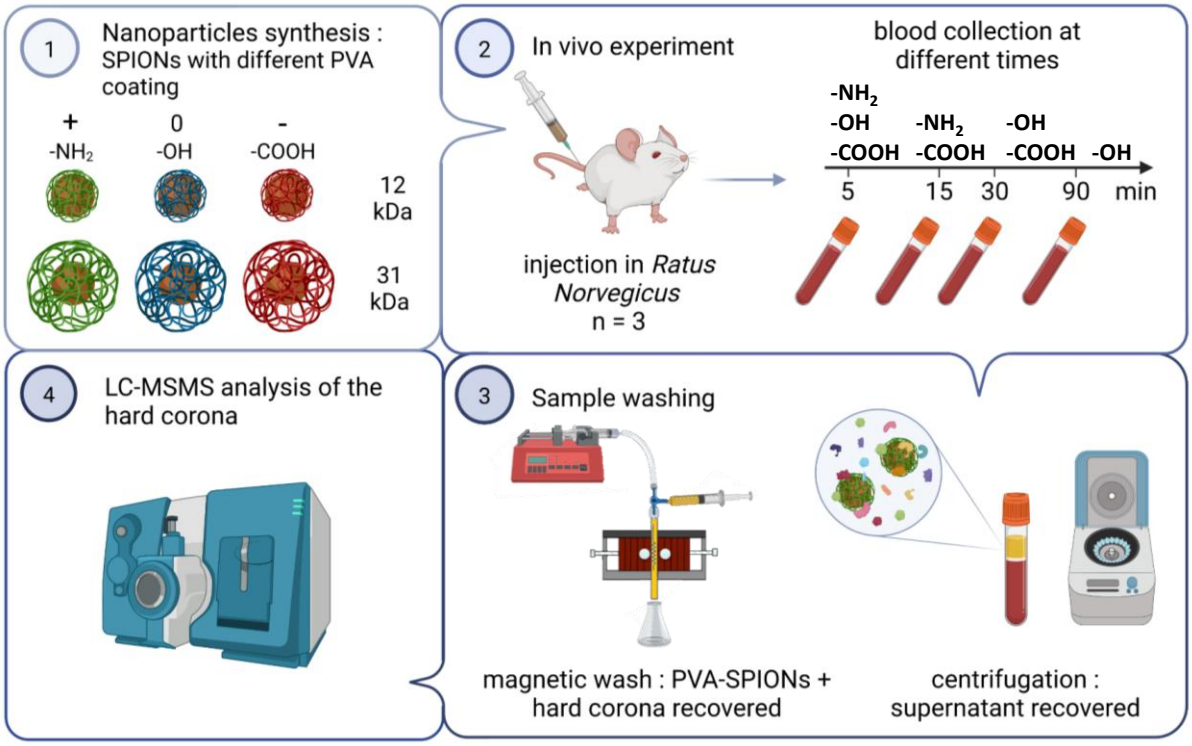

Figure 2. Schematic representation of the study workflow.

Identification of proteins adsorbed on the NPs over time

To identify the proteins determining NP circulation time, the corona compositions of NPs collected over different time points (chosen on the basis of pharmacokinetics properties of each NP) were characterized using LC-ESI-MS/MS. All samples have been weighted in mass of SPIONs to be able to compare and quantify each condition studied. The corona compositions of negatively charged NPs collected 5, 15, and 30 min after tail vein injection were identified, and those of positively charged NPs obtained 5 and 15 min after injection were studied. In the case of neutral SPIONs, thanks to their long circulation time, the corona compositions of NPs collected 5, 30, and 90 min after injection were identified (Table S3). SPIONs-PVA protein coronas were composed of 60 to 130 proteins (Figure 3a and b), in contrast to previous studies [35] where negatively-charged NPs adsorbed less different types of proteins compared to neutral and positive SPIONs-PVA. It is worth noticing that the 5 and 20 most abundant proteins correspond to approximately 30 % and 60 % of the total mass of detected proteins, respectively (Tables S4-S11). Thus, approximately only one fifth of the detected proteins corresponds to 60 % of the total amount of the protein corona. Similar trends were identified in previous studies by Sakulkhu et al [32, 35] where the 5 most abundant proteins correspond to between 20% and 60% of the total proteins detected, which emphasizes their significance to NPs pharmacokinetics.

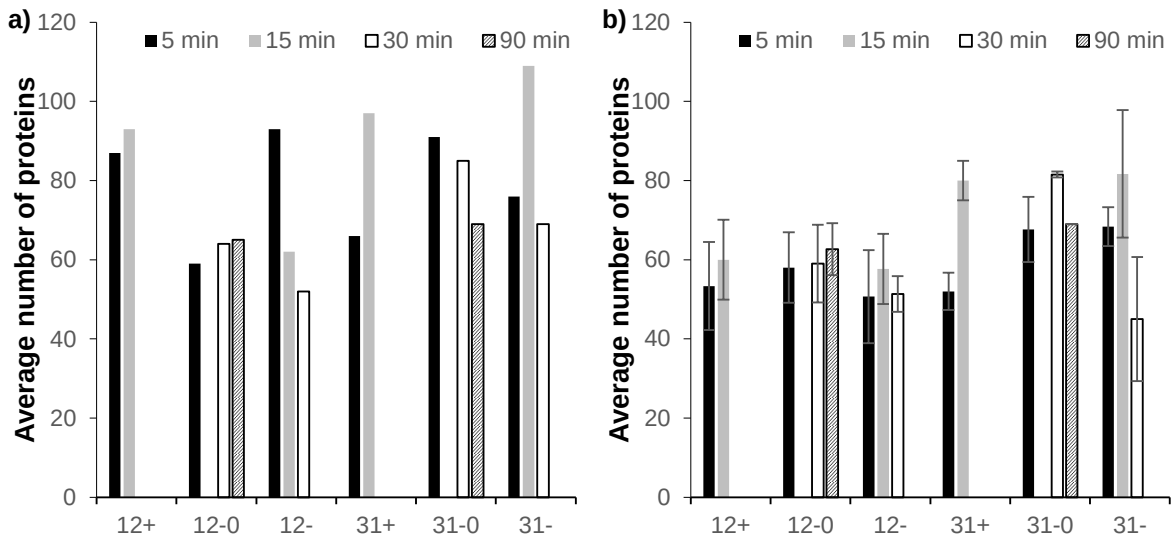

Figure 3. a) Number of all different proteins identified by LC-ESI-MS/MS at each time point and condition and b) average number of identified proteins at each time point and condition with error bars (duplicate experiments, triplicate analyses).

To understand how the NPs surface properties (charge and PVA molecular weight) influence the overall protein corona, we considered the physicochemical properties of each adsorbed protein. Namely, the grand average of hydropathy (GRAVY) score and isoelectric point (pI) of each detected protein were weighted according to their Normalized Spectral Count (NSpC), and an overall value of GRAVY and pI was calculated (Figure S4). The GRAVY and pI of all proteins present in the protein corona are almost similar. This is due to the combination of two factors: the numerous proteins detected - of around 100 proteins per NP and time point (Figure 3a and b) – and the physicochemical properties of those proteins. If we consider all time points and all NPs studied, we were able to identify 189 different proteins, with an average GRAVY of -0.35 ± 0.26 and an average pI of 6.55 ± 1.47 (figure S5). These values are very similar to the ones presented in Table S13. This suggests that most proteins found on the protein corona have similar physicochemical characteristics, regardless of the NPs size, charge and polymer MW.

In addition, the same rationale was applied for the 20 and 5 most abundant proteins found in the protein corona, since they corresponded to 60 % and 30 % of the total mass of detected proteins, respectively, as mentioned above (Figure 4 and Figure S6). These analyses showed that the GRAVY (hydrophobicity value) score of corona proteins adsorbed on all NPs changes over time. It indicates that the hydrophobicity/hydrophilicity of corona proteins formed on the NPs is dynamic and varies with time. Similarly, the pI (the pH at which the net charge of protein molecules is zero) of coronas formed on all NPs also changes with time. Depending on their charge and polymer length, NPs showed different trends of pI and GRAVY changes. Any alteration in GRAVY and pI of corona proteins is related to the corona protein composition/content changes resulting from protein attachment, detachment, and replacement over time.

The changes are more evident when focusing on the 5 most abundant proteins, with 12+ NPs presenting the highest pI and GRAVY of 7.5 and -0.15, respectively (Figure 4). Albumin is by far the most abundant protein in rodent plasma, accounting for almost 50 % of plasma proteins [36]. It is usually the most abundant protein in the corona, as shown in Tables S4-S11, with the exception of 12+ NPs at 5 min where hemoglobin (Hb) is the most abundant protein. We suggest the high rate of adsorption of Hb on 12+ NPs might be related to their faster clearance. Focusing on the 31+ NPs, also eliminated after 15 min, the influence of Hb on GRAVY and pI is not so clear, but hemoglobin is the second most adsorbed protein at 5 min (Table S8). Figure 5a displays the evolution of hemoglobin over time, showing a higher adsorption of Hb onto positive SPIONs-PVA, though it also shows a high adsorption of the protein onto 12- NPs.

Hb interaction with NPs depends on H-bonding and hydrophobic and electrostatic interactions.[37-40] Focusing on electrostatic interactions, it has been shown that negatively charge NPs interact with Hb leading to reversible changes on its secondary structure and preserving its functionality.[39] However, Hb interaction with positive charged NPs leads to heme degradation and promotes NP aggregation.[38, 40] Hb-induced NP aggregation may accelerate the NP clearance from blood circulation system. Heme degradation induces the production of reactive oxygen species and inflammatory mediators and activates innate immune cells such as macrophages and neutrophils.[41] Thus, even though both negative and positive NPs have affinity to hemoglobin (Figure 5a), positive NPs-hemoglobin complexes might stimulate the immune system following heme degradation.

In addition, haptoglobin is an acute phase protein that controls oxidative and inflammatory damages caused by free hemoglobin in the blood.[42, 43] This protein forms a complex with hemoglobin, which is then recognized by monocytes and macrophages.[42, 43] Figure S7 illustrates the evolution of haptoglobin overtime. While 12+ NPs adsorbed the highest amount of hemoglobin overtime (Figure 5a), 31+ NPs have the most haptoglobin that may bind to hemoglobin and stimulate NPs clearance by immune cells.

It is possible that the combination of Hb with other proteins affects the NP circulation time and other corona proteins strengthen or weaken the impact of Hb on shortening NP retention time. Therefore, different corona compositions of negatively and positively charged NPs might influence the effects of proteins governing NP circulation time. The protein structural changes caused by NPs can also affect their impact on NP circulation time. Further studies are required to understand the

mechanism by which corona proteins extend or shorten the NP retention in blood circulation.

Previous studies with similar NPs also suggested a higher absorption of Hb onto positively charged NPs (Table S12), particularly in an *in vivo* study involving Lewis rats where hemoglobin was the most abundant protein found in SPIONs-NH_2 hard corona [44]. Additionally, it showed that after 15 min, about half of the injected NPs were found in the liver, supporting that SPIONs-NH_2 have a fast clearance. Finally, Table S12 shows that hemoglobin was detected on the protein corona of the PVA-coated SPIONs incubated with FBS[35]. This is particularly important, since it demonstrates an affinity between hemoglobin and positively charged NPs, and that hemoglobin abundance is not related to red cells hemolysis. Hemoglobin is abundant on PVA-coated SPIONs. Further studies are required to understand the mechanism behind their interaction.

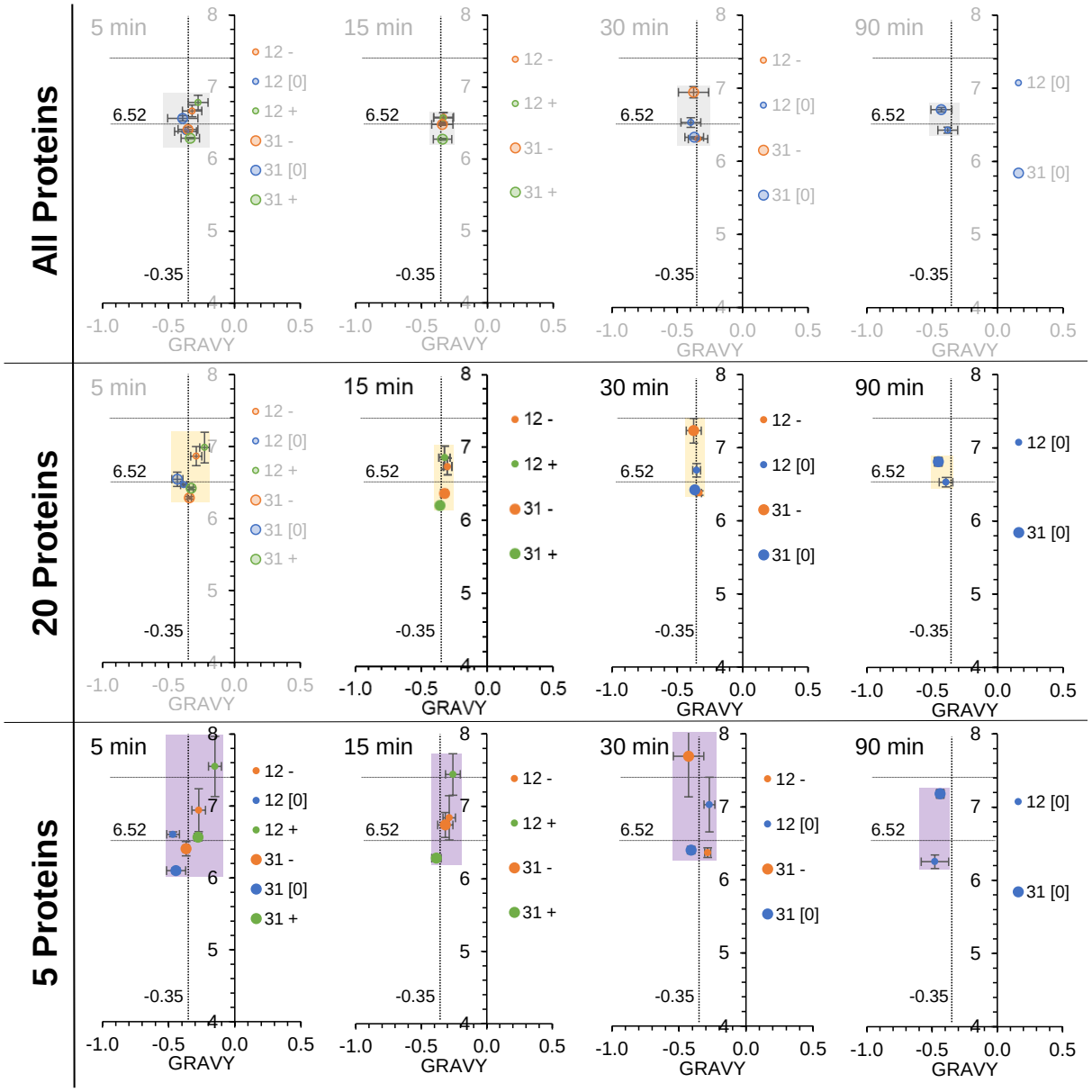

Figure 4. Comparison of the pI and GRAVY of a) total proteins, b) 20 most abundant proteins and c) 5 most abundant proteins adsorbed on the NPs over time. Squares represent the distribution of PI and GRAVY for each condition.

The adsorption of proteins onto the NP surface is a dynamic and competitive process. Hence, corona decoration may change over time. Tenzer *et al.* [45] showed that only the content/amount of proteins adsorbed on the NP surface changes over time, thus the composition/type of corona proteins is invariable. As mentioned before (Figure 4), the differences between physicochemical properties of NPs protein corona (GRAVY and pI) are more evident for the 5 most abundant proteins. Those

become less clear for the 20 most abundant proteins, while almost no differences can be found when considering all the proteins in the corona. In fact, the total proteins GRAVY and pI tends to - 0.35 and 6.52, respectively, independent on the charge, polymer MW or time point (Figure 4a and Table S13), which is in agreement with the findings by Tenzer *et al*.[45] Plus, this supports that any changes in corona protein content affect the biological impacts of NPs. Therefore, it is important to evaluate the amount of protein adsorbed on the NPs over time.

Some proteins such as albumin, fibrinogen, complement factors, immunoglobulin, apolipoproteins, and serotransferrin are dominantly adsorbed on the surface of most NPs entering biological media. Most of these proteins are opsonins/dysopsonins, which determine the retention time of NPs in blood circulation (Figure 5c). We calculated the amount of these proteins on the NP surface over time. According to the data obtained from LC-ESI-MS/MS analysis, the content of proteins (albumin, fibrinogen, complement factors, immunoglobulin, apolipoproteins, and serotransferrin) adsorbed onto the long- and short-circulating NPs was not significantly different (Figure 5 and Figure S8). Therefore, it is required to recognize the unknown biomolecules governing NP circulation time.

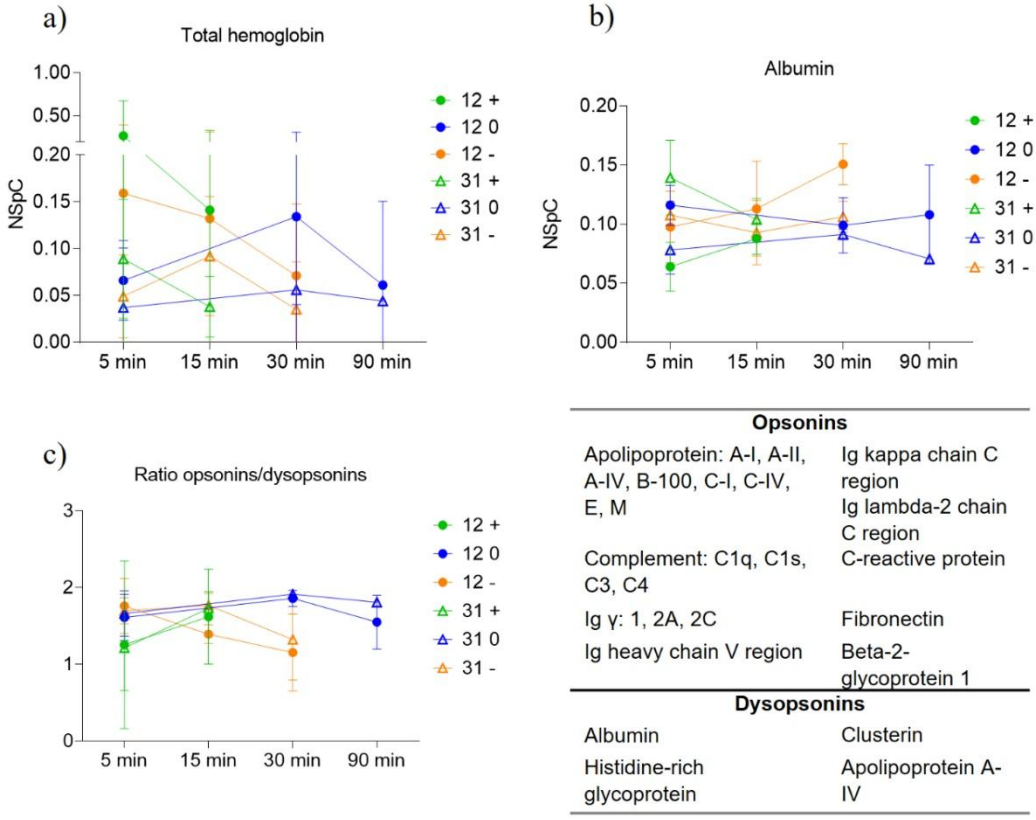

Opsonins	
Apolipoprotein: A-I, A-II, A-IV, B-100, C-I, C-IV, E, M	Ig kappa chain C region
	Ig lambda-2 chain C region
Complement: C1q, C1s, C3, C4	C-reactive protein
Ig γ: 1, 2A, 2C	Fibronectin
Ig heavy chain V region	Beta-2-glycoprotein 1
Dysopsonins	
Albumin	Clusterin
Histidine-rich glycoprotein	Apolipoprotein A-IV

Figure 5. Concentration changes of a) hemoglobin and b) albumin adsorbed on the NPs over time. c) Ratio of opsonins/dysopsonins adsorbed on the NPs over time. Total hemoglobin corresponds to the sum of NSpC of hemoglobin subunit alpha-1/2, hemoglobin subunit beta-1, and hemoglobin subunit beta-2.

Principal component analysis (PCA)

Although different NPs had similar opsonin/dysopsonin content, their blood circulation times were different. Therefore, it is possible that some NP-bound proteins, which have not yet been identified as key determinants of NP circulation time, govern the retention time of NPs in blood circulation system. This hypothesis was confirmed by calculating the ratio of opsonins/dysopsonins adsorbed onto the NPs. As can be seen in Figure 5c, the ratio of opsonins/dysopsonins adsorbed onto the neutral NPs was higher than that of negatively and positively charged NPs and

hence, it is expected that neutral NPs show the shortest blood circulation time. In contrast to what was expected, neutral NPs showed the longest blood circulation time, which suggests that unknown proteins determine the NP circulation time in the blood system. To identify these proteins, we compared the proteins adsorbed onto the NP surface over time.

To investigate whether the protein corona composition of different NPs could be representative of various circulation times for each group of NPs, we applied principal component analysis (PCA) to proteomic data on protein corona compositions of SPIONs-PVA (12 kDa and 31 kDa) (Figure 6). Details of the method are described in the Methods section.

Weighted-variable importance is introduced and applied for the ranking of variables based on the variances contributed by variables in each principal component in PCA analysis and loading plots. In this regard, top-ranked variables were selected, and we carefully looked at the variation of each variable (protein) over different time courses. Using this analysis, we recognized 24 proteins that are responsible for different circulation times of NPs in blood (Table 2). In agreement with previous reports[22, 46-48], most of the recognized proteins are opsonins/dysopsonins such as different types of apolipoproteins, complement factors, immunoglobulins, fibrinogen, and coagulation factors, which were previously introduced as the determining factors governing the NP circulation time in animal/human body. This result implies that our research plan and experiments are accurate and resulted in the identification of the proteins, which are responsible for NP circulation time.

Table 2. List of proteins governing NP retention time in blood circulation.

-	Alpha-2-HS-glycoprotein	-	Ficolin-1
-	Apolipoprotein A-I	-	Hemoglobin subunit alpha-1/2
-	Apolipoprotein A-II	-	Hemoglobin subunit beta-1
-	Apolipoprotein C-I	-	Hemoglobin subunit beta-2
-	Apolipoprotein E	-	Ig kappa chain C region, B allele
-	Coagulation factor VII	-	Lipoprotein lipase
-	Complement C3	-	Matrix Gla protein
-	Extracellular matrix protein 1	-	Metalloproteinase inhibitor 3
-	Fibrinogen alpha chain	-	Murinoglobulin-1
-	Fibrinogen beta chain	-	Osteopontin
-	Fibrinogen gamma chain	-	Secreted phosphoprotein 24
-	Fibronectin	-	Serine protease inhibitor A3K

According to the data obtained from LC-ESI-MS/MS and PCA analyses, the concentration of some proteins such as osteopontin, lipoprotein lipase, coagulation factor VII, matrix Gla protein, secreted phosphoprotein 24, alpha 2H glycoprotein, and apolipoprotein C-I was considerably high in the corona of long-circulating NPs, while the concentration of hemoglobin subunit beta was high in the corona of short-circulating NPs (Figure S9). These biomolecules are mainly involved in forming connective tissues, immune response, blood clotting and platelet activation, vascular and extracellular calcification, removing cholesterol, and oxygen transport

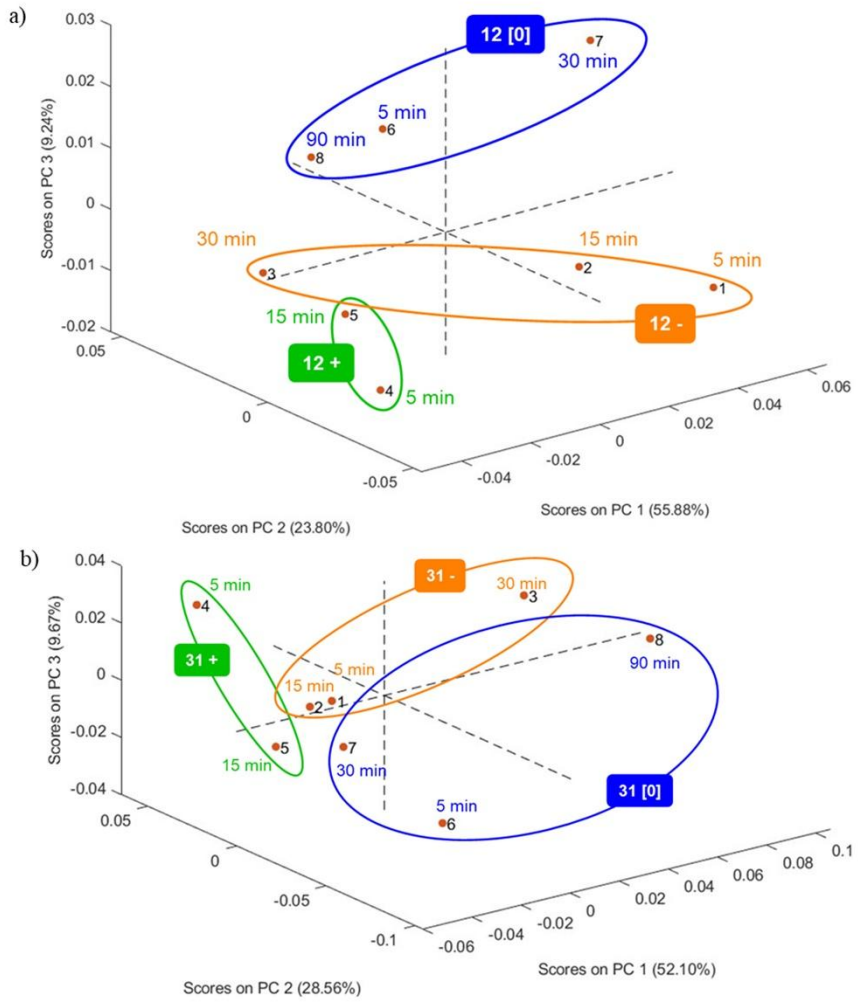

Figure 6. a) PCA profile of different coronas formed on the SPIONs-PVA 12 kDa negative at 5 min (1), 15 min (2), 30 min (3), SPIONs-PVA 12 kDa positive at 5 min (4), 15 min (5), SPIONs-PVA 12 kDa neutral at 5 min (6), 30 min (7), 90 min (8). b) PCA profile of different coronas formed on the SPIONs-PVA 31 kDa negative at 5 min (1), 15 min (2), 30 min (3), SPIONs-PVA 31 kDa positive at 5 min (4), 15 min (5), SPIONs-PVA 31 kDa neutral at 5 min (6), 30 min (7), 90 min (8).

(Table S14) [21, 49-55].

Most of these proteins are positively charged at physiological pH and hence, they are not adsorbed on positively charged NPs due to electrostatic repulsion (Table S15). Some of proteins, introduced here, such as alpha 2H glycoprotein can act as an opsonin or dysopsonin, depending on the NP charge [56]. It is also possible that the combination of different types of proteins determines the blood circulation time of NPs. Therefore, these proteins should be considered as determining factors governing the retention of NPs in blood circulation. Identifying new proteins governing NP circulation time provides a promising opportunity to control the NP circulation time *via* tuning corona decoration on the NP surface.

Pre-coating NPs with suitable proteins is an effective strategy to enrich them on the NP surface even after NPs are expose to biological media [57, 58]. It was shown that the targeting antibodies pre-adsorbed on the NP surface remained functional after exposure to plasma and were not completely replaced or masked by the protein corona [58]. While other plasma proteins are also adsorbed on the surface of pre-coated NPs, a high number of desired proteins that are precoated on the NPs can have a significant impact on NP circulation time. The pre-coating silica NPs with gamma-globulins (g-globulins) produced a protein corona that was enriched with opsonins, such as immunoglobulins [57].

It is also possible to tune the NP surface chemistry to specifically recruit desired proteins or reduce the adsorption of total proteins on their surfaces [59, 60]. For example, coating NPs with a zwitterionic structure has been reported as an effective strategy to reduce protein adsorption on the NPs [60]. The surface chemistry of nanocarriers can also be specified to modulate adsorbed albumin structure and thereby tune clearance by macrophage scavenger receptors [61]. Therefore, we can

specify the NP surface chemistry to adsorb desired proteins or modulate their structure to tune clearance by macrophages.

It is also possible to adsorb suitable proteins to improve the NP pharmacokinetics on the NP surface by tuning the density of PEG. For example, the enrichment of apolipoprotein A1 and clusterin occurred at the NPs covered by low concentration of PEG [62].

Furthermore, coating NPs with Poly-phosphoesthers (PPEs)-based surfactants is an effective strategy to reduce the adsorption of IgG and albumin and increase the attraction of a high amount of ApoA1 and clusterin on the NP surface [63]. These evidences highlight the importance of identifying the proteins governing NP circulation time in the development of nanomedicine and showed that precoating NPs with desired proteins and/or tuning NP surface chemistry can be as promising approaches to control the corona decoration on the NP surface and consequent NP half-life in blood circulation system.

In this study, we identified the hard corona proteins determining the NP retention time in the blood circulation system. There are some hidden factors in the nano-bio interfaces that should be considered and discussed when we study the corona protein's role in governing the plasma half-life of NPs.

Soft corona is a dynamic layer of biomolecules that have weak interaction with NPs and remain on their surfaces for a transient time [11]. Although this dynamic layer continuously changes over time, soft corona proteins might affect the NP-cell interaction and consequent NP retention time in the blood circulation system. To date, there is no technique to specifically isolate the soft corona, and methods such as *in situ* click-chemistry reaction and *in situ* Fishing do not accurately isolate the

whole soft corona proteins [64, 65]. Therefore, we preferred to study the hard corona proteins, which have a long-term residency on the NPs, and their role in NP retention time in the blood circulation system.

The NP surface is immediately covered by biomolecules when they enter the biological media. The current assumption is that the protein corona fully covers the NP surface in seconds. However, it's possible that the surface charge of some parts that are not covered by biomolecules affects the NP-cell interaction and their biological fate.

Protein corona maturation and hardening refers to the process by which the corona proteins on the surface of NPs undergo structural changes or reorientation and become more stable over time [66, 67]. The proteins adsorbed on the NPs may undergo structural changes that lead to the exposure of cryptic epitopes that affect the NP-cell interaction and NP circulation time and biodistribution [68]. It's so hard to probe the conformation of a specific protein in a mixture of hundreds of proteins adsorbed on the NPs. Using fluorescence resonance energy transfer (FRET)-labeled fibronectin (FN), we tracked the conformational changes of FN located in the hard corona and soft corona [69]. We showed that the labeled FN proteins, which directly attached to the gold NP surface (hard corona), underwent more severe conformational changes than those associated with the protein corona *via* protein-protein interactions (soft corona). Therefore, soft corona proteins that face the cells undergo the least structural changes and the NP-induced protein structural change may not considerably affect the NP circulation time. Further analyses are required to determine the possible effects of corona protein structural changes on the NP retention time in the blood circulation system.

CONCLUSION

In this paper, we studied the role of surface chemistries, especially charges and polymer lengths on the plasma half-lives of SPIONs and linked the biological results to the composition of *in vivo* protein coronas formed on the NP surfaces. As plasma half-life does not appear to be linked to the lengths of the polymers but only to their charges, the compositions of protein coronas formed on 12 and 31 kDa coated SPIONs were only slightly different. NPs with different circulation times adsorbed similar types/levels of opsonins/dysopsonins, which are usually known as crucial determining factors for NP circulation time. With accurate data analyses, we discovered a cocktail of proteins that might be responsible for the long circulation time of NPs: osteopontin, lipoprotein lipase, coagulation factor VII, matrix Gla protein, secreted phosphoprotein 24, alpha 2H glycoprotein, and apolipoprotein C-I, while hemoglobin seems to shorten blood clearance. Concentrating on these new proteins might be essential to understand and possibly tune NPs surfaces to extend circulation time, by avoiding the RES uptake. Identification of the proteins directing NP circulation time is a critical step for controlling NP behavior and fate in the human body. Measuring protein adsorbed on NPs *in vivo* remains a challenge, as there are many parameters that can influence and bias results. Some solutions to improve accuracy might be to: i) try standardizing protein corona analyses such as by having a consensus on how to select and isolate the hard corona ; and ii) by automating proteins separations [70] to avoid bias due to the different methods used by operators.

METHODS

Materials. Iron(III) chloride hexahydrate ($FeCl_3$*$6H_20$, 98-102%, CAS 10025-77-1, Sigma-Aldrich) ; Iron(II) chloride tetrahydrate ($FeCl_2$*$4H_20$, >99%, CAS 13478-10-9,

Sigma-Aldrich) ; Ammonium Hydroxide 28% ; Nitric acid 65% ; NaCl, Polyvinyl alcohols ; PVA Mowiol 3-85 (12 kDa); M12 (NH_2 functionalized: 80140 kDa); KL506 (COOH functionalized: 30-50 kDa) from Kuraray. PVA Mowiol 4-88 (31 kDa) from Merck Fetal Bovin Serum FBS was purchased from Sigma Aldrich.

NPs synthesis & functionalization. SuperParamagnetic Iron oxide nanoparticle (SPIONs) were synthetized *via* a coprecipitation method previously described [71, 72]. Polyvinyl alcohol (PVA) solutions were prepared in NaCl 0.15M solution at different concentrations: PVA 3-85, 4-88 and KL506 at 100 mg/mL and PVA M12 at 20 mg/mL. SPIONs-PVA with different surface characteristics were obtained by mixing naked SPIONs suspensions and the PVA solutions. For Neutral SPIONs-PVA called SPIONs-PVA_{12}-OH (12[0]) and SPIONs-PVA_{31}-OH (31[0]), 5 mL of naked SPIONs were mixed with 0.5 mL of NaCl 0.15M and 4.5 mL of solution of PVA 3-85 or PVA 4-88 respectively. For negatively charged SPIONs-PVA called SPIONs-PVA_{12}-COOH (12-) and SPIONs-PVA_{31}-COOH (31-), 5 mL of naked SPIONs were mixed with 0.5 mL of NaCl 0.15M, 2.25 mL of KL506 solution and 2.25 mL of a solution of PVA 3-85 or PVA 4-88 respectively. For positively charged SPIONs-PVA called SPIONs-PVA_{12}-NH_2 (12+) and SPIONs-PVA_{31}-NH_2 (31+), 5 mL of naked SPIONs were mixed with 0.5 mL of the solution of M12 and 4.5 mL of a solution of PVA 3-85 or PVA 4-88 respectively. SPIONs-PVA suspensions (at 5 mg_{SPIONs}/mL) were stored at 4°C at least one week before use and pH was adjusted to 7.4 with NaOH prior to biological experiments.

NPs characterization. Electronic microscopy images were acquired on a TEM from Hitachi (HT7800 with 120 kV LaB6 electron gun). TEM diameter (dTEM) was obtained by counting diameter of 400 crystallites. The hydrodynamic diameter (dH), polydispersity index (PDI) and zeta potential were measured by DLS and

Electrophoretic Light Scattering (ELS) (Zetasizer nano-ZS, Malvern Panalytical, Malvern, UK). The Zetasizer was equipped with a red 633 nm He–Ne laser and measurements were performed at a 173° degree scattering angle. All measurements were performed at 25 °C. The refractive index (RI) and the value for the viscosity of iron oxide (2.420; 0.887 cP) were used. The laser power-attenuator was adjusted automatically.

Size and zeta potential measurements were performed in triplicate (n=3) in DTS1070 reusable cuvettes, after sample dilution. SPIONs suspensions were diluted in NaCl 0.15 M at pH 7.4 and FBS (30 times dilution). For naked SPIONs and SPIONs-PVA, only dH in intensity were reported to compare sizes before and after incubation in proteins. Indeed, dH in number reflects mainly the size of the proteins in that case because they outnumber NPs. For Zeta potential, suspensions were also diluted 30 times in NaCl 10^{-2} M at pH 7.4. Peak 1 mean, PDI and zeta potential were determined and data were analyzed by Malvern Instruments Zetasizer Software version 7.12.

NPs concentration. SPIONs concentrations in suspension and in plasma were determined *via* magnetic susceptibility measurements using a MS2G single frequency sensor magnetic susceptibility meter from Bartington Instruments [73].

Animals. Wistar female rats (Charles River, France, 210-230 g) were housed 7 days before the start of the experiments and were maintained in a day/night cycle of 12 hours. These experiments were conducted following the legislation on the use of laboratory animals (directive 2010/63/EU) and have been approved by the accredited ethics committee (C2ea Grand Campus n°105).

In vivo injection of NPs. Rats were anesthetized with isoflurane (2-2,5%) on warm plate. They were injected in the tail vein with 1 mL at 5 mg_{NPs}/mL of the 6 different SPIONs-PVA.

Determination of SPIONs-PVA bio-circulation half-lives. After injection, 200 µL blood samples were taken out at different time points: 5, 10, 20, 30, 45, 60, 90 and 120 and / or 240 min depending on the live observations of SPIONs concentrations. Each 200µL sample was diluted to 600µL in physiological serum with heparin (50 UI / mL) and measured with magnetic susceptibility to get SPIONs' concentrations. Half-lives were obtained by plotting the evolution of SPIONs' concentrations compared to the initial concentration (in % of injected dose) as a function of the sampling times. Experiments were conducted on biological duplicates and measurements' triplicate. The mathematical model used to fit all the data points provided the half-lives and their absolute error.

Blood samples collections. After half-life times were determined, another experiment was conducted to select and analyze the protein corona adsorbed on the different SPIONs-PVA. Rats were injected with 1 mL of the 6 same SPIONs-PVA described before and 600 µL blood samples were collected at different time points depending on the NPs' charge : 5 and 15 minutes for positives ones, 5 - 15 - 30 minutes for negative, 5 - 30 - 90 minutes for neutral ones. The samples as such were then centrifuged (10min, 3000 g, 4°C). Supernatants, containing plasmas with NPs were delicately collected and their SPIONs' concentrations were measured 3 times in magnetic susceptibility. NPs/proteins complexes were then isolated by passing through a hollow magnetic reactor[44], rinsed with 5 mL of PBS, followed by a second wash with 5mL PBS + NaCl 2M. The syringe pump was set up at 1 mL / min following previously described protocol[44, 74]. This protocol was optimized to be able to

remove the low adsorbed proteins called the soft corona to only focus on the strongly adsorbed proteins: the hard corona[11]. With 2 times 10 columns washings, only the hard corona was selected and analyzed. Samples were stored at -80°C. Each experimentation was conducted on three different rats.

ESI-LC-MSMS sample preparation. SPIONs with proteins were sonicated during 15 min at room temperature in an ultrasonic bath, then 30 sec in an ultrasonic processor for vial (amplitude 70, cycle 0.5). For each batch of sample, the same amount of NPs was taken from each samples and diluted to 300 µl with NaCl 2M in PBS (see supplemental information section). 6 µl of Dithioerythritol (DTE) 50 mM in distilled water were added then reduction was carried out at 37°C for 1h. Alkylation was performed by adding 6 µl of iodoacetamide (400 mM in distilled water) during 1 hour at room temperature in the dark. Overnight digestion was performed at 37 °C with 6 µL of freshly prepared trypsin (Promega) at 0.1 µg/µl in acetic acid. Samples were completely dried under speed-vacuum and then desalted with a C18 microspin column (Harvard Apparatus, Holliston, MA, USA) according to manufacturer's instructions. Samples were finally completely dried under speed-vacuum and stored at -20°C.

ESI-LC-MSMS experimentation. Analyses were conducted on a nanoLC-MSMS using an easynLC1000 (Thermo Fisher Scientific) coupled with a Q-Exactive HF mass spectrometer (Thermo Fisher Scientific). Samples were diluted in 10 µl of loading buffer (5% CH3CN, 0.1% FA) and 5 µl were injected on column. LC-ESI-MS/MS was performed on a Q-Exactive HF Hybrid Quadrupole-Orbitrap Mass Spectrometer (Thermo Fisher Scientific) equipped with an Easy nLC 1000 liquid chromatography system (Thermo Fisher Scientific). Peptides were trapped on a Acclaim pepmap100, C18, 3µm, 75µm x 20mm nano trap-column (Thermo Fisher Scientific) and

separated on a 75 µm x 250 mm, C18, 2µm, 100 Å Easy-Spray column (Thermo Fisher Scientific). The analytical separation was run for 40 min using a gradient of H_2O/FA 99.9%/0.1% (solvent A) and CH_3CN/FA 99.9%/0.1% (solvent B). The gradient was run as follows: 0-5 min 95 % A and 5 % B, then to 65 % A and 35 % B for 25 min, and 10 % A and 90 % B for 10 min at a flow rate of 250 nL/min. Full scan resolution was set to 60'000 at m/z 200 with an AGC target of 3 x 106 and a maximum injection time of 60 ms. Mass range was set to 400-2000 m/z. For data dependent analysis, up to twenty precursor ions were isolated and fragmented by high energy collisional dissociation HCD at 27% NCE. Resolution for MS2 scans was set to 15'000 at m/z 200 with an AGC target of 1 x 105 and a maximum injection time of 60 ms. Isolation width was set at 1.6 m/z. Full MS scans were acquired in profile mode whereas MS2 scans were acquired in centroid mode. Dynamic exclusion was of 20s.

ESI-LC-MSMS database research. Peak lists (MGF file format) were generated from raw data using the MS Convert conversion tool from ProteoWizard. The peaklist files were searched against the Rattus Norvegicus Reference Proteome (uniprot.org, release 01_2021, 8125 entries) combined with an in-house database of common contaminant using Mascot (Matrix Science, London, UK; version 2.5.1). Trypsin was selected as the enzyme, with one potential missed cleavage. Precursor ion tolerance was set to 10 ppm and fragment ion tolerance to 0.02 Da. Carbamidomethyl of cysteine was specified as fixed modification. Deamidation of asparagine and glutamine, and oxidation of methionine were specified as variable modifications. The Mascot search was validated using Scaffold 5.0.0 (Proteome Software). Peptide identifications were accepted if they could be established at a probability to achieve an FDR less than 0.1 % by the Percolator posterior error probability calculation (Käll,

L et al, Bioinformatics, 24(16):i42-i48, Aug 2008). Protein identifications were accepted if they could be established at a PCF | [October 27, 2021] 5 probability to achieve an FDR less than 1.0 % and contained at least 2 identified peptides. Protein probabilities were assigned by the Protein Prophet algorithm (Nesvizhskii, Al et al Anal. Chem. 2003;75(17):4646-58). Proteins that contained similar peptides and could not be differentiated based on MS/MS analysis alone were grouped to satisfy the principles of parsimony.

LC-MS Data analysis. Normalized Spectral Count (NSpC) were normalized using the classical formula : $NSpC_k = \frac{\left(\frac{TSC}{MW}\right)_k}{\sum_{i=0}^{N} TSC_i/MW_i}$ with NSpC the normalized TSC (total spectra count) of a protein k, MW the molecular weight (kDa). All LC-MS data were run in triplicate and their standard deviations were added on the different graphs.

Principal component analysis (PCA). In this work, we used principal component analysis as an unsupervised method to represent a high-dimensional data structure in a smaller number of dimensions and to find the variables that have more weight for characterizing objects in a data set. In this way we can observe groupings of objects and outliers which define the structure of the data set. Our data points for two SPION particles (12kDa and 31kDa) in different charges, cationic, neutral, and anionic, were separated into two sets. PCA analysis was performed on each set, the first three eigenvalues explained more than 85 % of the total variance. Based on the weights (loadings plot) in absolute value of the variables for the first three principal components, we selected those variables that had a loading higher than 0.2 for each set as important variables (proteins) affecting blood circulation time.

Acknowledgments

This work was performed within Pharm'Image, a regional center of excellence in Pharmacoimaging. Support was provided by the French Government through the French National Research Agency (ANR) under the program "Investissements d'Avenir" (ANR-10-EQPX-05-01/IMAPPI Equipex) and the CNRS, the "Université de Bourgogne" and the "Conseil Régional de Bourgogne" This work is also part of the project "Pharmacoimagerie et agents théranostiques", funded by the "Université de Bourgogne" and the "Conseil Régional de Bourgogne" through the "Plan d'Actions Régional pour l'Innovation (PARI)" and the European Union through the PO FEDER-FSE Bourgogne 2014/2020 programs. Authors also would like to acknowledge the supports of EIPHI Graduate School (contract ANR-17-EURE-0002), the ANER project "Nanoprot" n° 2019-Y-10648 and the ANR Nanoblorona (contract ANR-21-CE18-0015). Authors would like to thank the France-Stanford center through the France-Stanford collaborative project for their support.

The authors would like to thank A. Hainard from the Proteomics Core Facility of the University of Geneva (Switzerland) for LC-ESI-MS/MS analyses and R. Chassagnon form the department ARCEN (Applications, Research and Characterization at Nanoscale) of the laboratory ICB for the TEM pictures.

Supporting Information

Supporting information available:

- Characterizations of the nanoparticles (TEM pictures of naked and PVA-coated SPIONs, DLS, and zeta potential measurements in serum).
- Experimental procedures in vivo and time of collections of in vivo samples.
- List of 5 and 20 most abundant proteins at different times of collection and different surface functionalization

- Example of calculation of the overall protein corona GRAVY and pI

- GRAVY and pI repartitions of the 189 proteins identified

- Comparison of the GRAVY and the pI of the 5 and 20 most abundant proteins and all the proteins found at different times on SPIONs-PVA with the same charges.

- Evolution of haptoglobin on NPs surface over time

- Hemoglobin content of the corona adsorbed in NPs over time; GRAVY and pI of the proteins of each time point and NPs surfaces

- Evolutions of serotransferrin, complement C3, total IgG, total complement, total apolipoproteins, and total fibrinogen adsorbed on NPs at different time points and surface functionalization.

- Time evolution of the amount of proteins extending NPS circulation time

- Physiological functions of identified proteins in this study

- GRAVY and pI of proteins extending the circulation time

Author Contributions

Study design: L. M. (conception of study), A. O. (pharmacokinetics study), Ce. M., L. S. and L. M. (particle synthesis and characterization), Ci. M., O. J., G. B. and L. M. (proteins analyses), Ci. M. M. H., R. S. and L. M. (proteomics results exploitation)

SPION synthesis, functionalization and characterization: Ce. M, L. S. and L.M.

Pharmacokinetic *in vivo* studies: Ce. M., A. O. and L. M

Proteins analyses: Ci. M., G. B. and O. J.

Proteins results exploitation: Ci. M., M. H., Ce. M., R. S. and L. M.

Authors who analyzed the data and prepared figures for their respective experiments. Writing – Original Draft Preparation: Ci. M., M. H. and L. M.; Writing – Review & Editing: all authors; Funding Acquisition: O. J. and L. M.

TOC figur

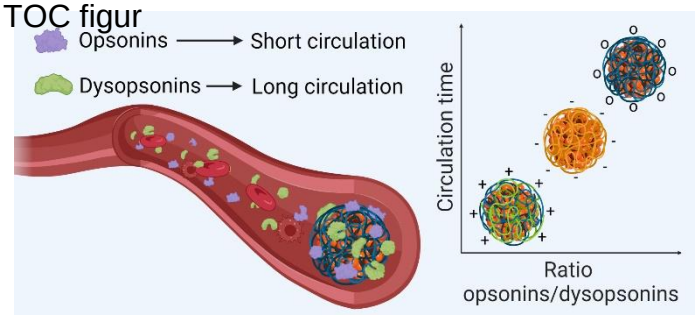
Opsonins
Short circulation
Dysopsonins
Long circulation
Circulation time
Ratio
opsonins/dysopsonins

REFERENCES

1. Lammers, T.; Kiessling, F.; Ashford, M.; Hennink, W.; Crommelin, D.; Storm, G., Cancer nanomedicine: is targeting our target? *Nature Reviews Materials* **2016,** *1* (9), 1-2.
2. Hajipour, M. J.; Fromm, K. M.; Ashkarran, A. A.; de Aberasturi, D. J.; de Larramendi, I. R.; Rojo, T.; Serpooshan, V.; Parak, W. J.; Mahmoudi, M., Antibacterial properties of nanoparticles. *Trends in biotechnology* **2012,** *30* (10), 499-511.
3. Moabelo, K. L.; Martin, D. R.; Fadaka, A. O.; Sibuyi, N. R.; Meyer, M.; Madiehe, A. M., Nanotechnology-based strategies for effective and rapid detection of SARS-CoV-2. *Materials* **2021,** *14* (24), 7851.
4. Ling, D.; Hackett, M. J.; Hyeon, T., Surface ligands in synthesis, modification, assembly and biomedical applications of nanoparticles. *Nano Today* **2014,** *9* (4), 457-477.
5. Han, X.; Xu, K.; Taratula, O.; Farsad, K., Applications of nanoparticles in biomedical imaging. *Nanoscale* **2019,** *11* (3), 799-819.
6. Salvati, A.; Pitek, A. S.; Monopoli, M. P.; Prapainop, K.; Bombelli, F. B.; Hristov, D. R.; Kelly, P. M.; Åberg, C.; Mahon, E.; Dawson, K. A., Transferrin-functionalized nanoparticles lose their targeting capabilities when a biomolecule corona adsorbs on the surface. *Nature nanotechnology* **2013,** *8* (2), 137-143.
7. Dawson, K. A.; Yan, Y., Current understanding of biological identity at the nanoscale and future prospects. *Nature nanotechnology* **2021,** *16* (3), 229-242.
8. Ke, P. C.; Lin, S.; Parak, W. J.; Davis, T. P.; Caruso, F., A decade of the protein corona. *ACS nano* **2017,** *11* (12), 11773-11776.
9. Carrillo-Carrion, C.; Carril, M.; Parak, W. J., Techniques for the experimental investigation of the protein corona. *Current Opinion in Biotechnology* **2017,** *46*, 106-113.
10. Hajipour, M. J.; Safavi-Sohi, R.; Sharifi, S.; Mahmoud, N.; Ashkarran, A. A.; Voke, E.; Serpooshan, V.; Ramezankhani, M.; Milani, A. S.; Landry, M. P., An Overview of Nanoparticle Protein Corona Literature. *Small* **2023**, 2301838.
11. Walkey, C. D.; Chan, W. C., Understanding and controlling the interaction of nanomaterials with proteins in a physiological environment. *Chemical Society Reviews* **2012,** *41* (7), 2780-2799.
12. Singh, N.; Marets, C.; Boudon, J.; Millot, N.; Saviot, L.; Maurizi, L., *In vivo* protein corona on nanoparticles: does the control of all material parameters orient the biological behavior? *Nanoscale Advances* **2021,** *3* (5), 1209-1229.
13. Hajipour, M. J.; Laurent, S.; Aghaie, A.; Rezaee, F.; Mahmoudi, M., Personalized protein coronas: a "key" factor at the nanobiointerface. *Biomaterials science* **2014,** *2* (9), 1210-1221.
14. Cai, R.; Chen, C., The crown and the scepter: roles of the protein corona in nanomedicine. *Advanced Materials* **2019,** *31* (45), 1805740.
15. Hadjidemetriou, M.; McAdam, S.; Garner, G.; Thackeray, C.; Knight, D.; Smith, D.; Al-Ahmady, Z.; Mazza, M.; Rogan, J.; Clamp, A., The human *in vivo* biomolecule corona onto PEGylated liposomes: a proof-of-concept clinical study. *Advanced Materials* **2019,** *31* (4), 1803335.
16. Hajipour, M. J.; Raheb, J.; Akhavan, O.; Arjmand, S.; Mashinchian, O.; Rahman, M.; Abdolahad, M.; Serpooshan, V.; Laurent, S.; Mahmoudi, M., Personalized disease-specific protein corona influences the therapeutic impact of graphene oxide. *Nanoscale* **2015,** *7* (19), 8978-8994.
17. Lotfabadi, A.; Hajipour, M. J.; Derakhshankhah, H.; Peirovi, A.; Saffar, S.; Shams, E.; Fatemi, E.; Barzegari, E.; Sarvari, S.; Moakedi, F., Biomolecular corona dictates Aβ fibrillation process. *ACS chemical neuroscience* **2018,** *9* (7), 1725-1734.
18. Bertrand, N.; Grenier, P.; Mahmoudi, M.; Lima, E. M.; Appel, E. A.; Dormont, F.; Lim, J.-M.; Karnik, R.; Langer, R.; Farokhzad, O. C., Mechanistic understanding of *in vivo* protein corona formation on polymeric nanoparticles and impact on pharmacokinetics. *Nature communications* **2017,** *8* (1), 777.

19. Fedeli, C.; Segat, D.; Tavano, R.; Bubacco, L.; De Franceschi, G.; de Laureto, P. P.; Lubian, E.; Selvestrel, F.; Mancin, F.; Papini, E., The functional dissection of the plasma corona of SiO_2-NPs spots histidine rich glycoprotein as a major player able to hamper nanoparticle capture by macrophages. *Nanoscale* **2015,** *7* (42), 17710-28.
20. Ritz, S.; Schöttler, S.; Kotman, N.; Baier, G.; Musyanovych, A.; Kuharev, J.; Landfester, K.; Schild, H.; Jahn, O.; Tenzer, S.; Mailänder, V., Protein corona of nanoparticles: distinct proteins regulate the cellular uptake. *Biomacromolecules* **2015,** *16* (4), 1311-21.
21. Schöttler, S.; Becker, G.; Winzen, S.; Steinbach, T.; Mohr, K.; Landfester, K.; Mailänder, V.; Wurm, F. R., Protein adsorption is required for stealth effect of poly(ethylene glycol)- and poly(phosphoester)-coated nanocarriers. *Nat Nanotechnol* **2016,** *11* (4), 372-7.
22. Abbina, S.; Takeuchi, L. E.; Anilkumar, P.; Yu, K.; Rogalski, J. C.; Shenoi, R. A.; Constantinescu, I.; Kizhakkedathu, J. N., Blood circulation of soft nanomaterials is governed by dynamic remodeling of protein opsonins at nano-biointerface. *Nature communications* **2020,** *11* (1), 3048.
23. Tekie, F. S. M.; Hajiramezanali, M.; Geramifar, P.; Raoufi, M.; Dinarvand, R.; Soleimani, M.; Atyabi, F., Controlling evolution of protein corona: A prosperous approach to improve chitosan-based nanoparticle biodistribution and half-life. *Scientific reports* **2020,** *10* (1), 1-14.
24. Anselmo, A. C.; Kumar, S.; Gupta, V.; Pearce, A. M.; Ragusa, A.; Muzykantov, V.; Mitragotri, S., Exploiting shape, cellular-hitchhiking and antibodies to target nanoparticles to lung endothelium: Synergy between physical, chemical and biological approaches. *Biomaterials* **2015,** *68*, 1-8.
25. Hu, C.-M. J.; Fang, R. H.; Wang, K.-C.; Luk, B. T.; Thamphiwatana, S.; Dehaini, D.; Nguyen, P.; Angsantikul, P.; Wen, C. H.; Kroll, A. V., Nanoparticle biointerfacing by platelet membrane cloaking. *Nature* **2015,** *526* (7571), 118-121.
26. Zhou, H.; Fan, Z.; Li, P. Y.; Deng, J.; Arhontoulis, D. C.; Li, C. Y.; Bowne, W. B.; Cheng, H., Dense and dynamic polyethylene glycol shells cloak nanoparticles from uptake by liver endothelial cells for long blood circulation. *ACS nano* **2018,** *12* (10), 10130-10141.
27. Alberg, I.; Kramer, S.; Schinnerer, M.; Hu, Q.; Seidl, C.; Leps, C.; Drude, N.; Möckel, D.; Rijcken, C.; Lammers, T., Polymeric nanoparticles with neglectable protein corona. *Small* **2020,** *16* (18), 1907574.
28. Zhang, S.-q.; Fu, Q.; Zhang, Y.-j.; Pan, J.-x.; Zhang, L.; Zhang, Z.-r.; Liu, Z.-m., Surface loading of nanoparticles on engineered or natural erythrocytes for prolonged circulation time: strategies and applications. *Acta Pharmacologica Sinica* **2021,** *42* (7), 1040-1054.
29. Yoo, J.-W.; Chambers, E.; Mitragotri, S., Factors that control the circulation time of nanoparticles in blood: challenges, solutions and future prospects. *Current pharmaceutical design* **2010,** *16* (21), 2298-2307.
30. Tsoi, K. M.; MacParland, S. A.; Ma, X.-Z.; Spetzler, V. N.; Echeverri, J.; Ouyang, B.; Fadel, S. M.; Sykes, E. A.; Goldaracena, N.; Kaths, J. M., Mechanism of hard-nanomaterial clearance by the liver. *Nature materials* **2016,** *15* (11), 1212-1221.
31. Cho, W.-S.; Cho, M.; Jeong, J.; Choi, M.; Han, B. S.; Shin, H.-S.; Hong, J.; Chung, B. H.; Jeong, J.; Cho, M.-H., Size-dependent tissue kinetics of PEG-coated gold nanoparticles. *Toxicology and applied pharmacology* **2010,** *245* (1), 116-123.
32. Sakulkhu, U.; Maurizi, L.; Mahmoudi, M.; Motazacker, M.; Vries, M.; Gramoun, A.; Beuzelin, M.-G. O.; Vallée, J.-P.; Rezaee, F.; Hofmann, H., Ex situ evaluation of the composition of protein corona of intravenously injected superparamagnetic nanoparticles in rats. *Nanoscale* **2014,** *6* (19), 11439-11450.
33. Yamamoto, Y.; Nagasaki, Y.; Kato, Y.; Sugiyama, Y.; Kataoka, K., Long-circulating poly (ethylene glycol)–poly (d, l-lactide) block copolymer micelles with modulated surface charge. *Journal of controlled release* **2001,** *77* (1-2), 27-38.
34. Xiao, K.; Li, Y.; Luo, J.; Lee, J. S.; Xiao, W.; Gonik, A. M.; Agarwal, R. G.; Lam, K. S., The effect of surface charge on *in vivo* biodistribution of PEG-oligocholic acid based micellar nanoparticles. *Biomaterials* **2011,** *32* (13), 3435-3446.

35. Sakulkhu, U.; Mahmoudi, M.; Maurizi, L.; Coullerez, G.; Hofmann-Amtenbrink, M.; Vries, M.; Motazacker, M.; Rezaee, F.; Hofmann, H., Significance of surface charge and shell material of superparamagnetic iron oxide nanoparticle (SPION) based core/shell nanoparticles on the composition of the protein corona. *Biomaterials science* **2015,** *3* (2), 265-278.
36. Zaias, J.; Mineau, M.; Cray, C.; Yoon, D.; Altman, N. H., Reference values for serum proteins of common laboratory rodent strains. *Journal of the American Association for Laboratory Animal Science* **2009,** *48* (4), 387-390.
37. Chakraborty, M.; Paul, S.; Mitra, I.; Bardhan, M.; Bose, M.; Saha, A.; Ganguly, T., To reveal the nature of interactions of human hemoglobin with gold nanoparticles having two different morphologies (sphere and star-shaped) by using various spectroscopic techniques. *Journal of Photochemistry and Photobiology B: Biology* **2018,** *178*, 355-366.
38. Yang, H.; Hao, C.; Nan, Z.; Sun, R., Bovine hemoglobin adsorption onto modified silica nanoparticles: Multi-spectroscopic measurements based on kinetics and protein conformation. *International journal of biological macromolecules* **2020,** *155*, 208-215.
39. Devineau, S.; Zargarian, L.; Renault, J. P.; Pin, S., Structure and function of adsorbed hemoglobin on silica nanoparticles: relationship between the adsorption process and the oxygen binding properties. *Langmuir* **2017,** *33* (13), 3241-3252.
40. Mobasherat Jajroud, S. Y.; Falahati, M.; Attar, F.; Khavari-Nejad, R. A., Human hemoglobin adsorption onto colloidal cerium oxide nanoparticles: A new model based on zeta potential and spectroscopy measurements. *Journal of Biomolecular Structure and Dynamics* **2018,** *36* (11), 2908-2916.
41. Dutra, F. F.; Bozza, M. T., Heme on innate immunity and inflammation. *Frontiers in pharmacology* **2014,** *5*, 115.
42. Asleh, R.; Marsh, S.; Shilkrut, M.; Binah, O.; Guetta, J.; Lejbkowicz, F.; Enav, B.; Shehadeh, N.; Kanter, Y.; Lache, O., Genetically determined heterogeneity in hemoglobin scavenging and susceptibility to diabetic cardiovascular disease. *Circulation research* **2003,** *92* (11), 1193-1200.
43. Minović, I.; Eisenga, M. F.; Riphagen, I. J.; van den Berg, E.; Kootstra-Ros, J.; Frenay, A.-R. S.; van Goor, H.; Rimbach, G.; Esatbeyoglu, T.; Levy, A. P., Circulating haptoglobin and metabolic syndrome in renal transplant recipients. *Scientific reports* **2017,** *7* (1), 14264.
44. Sakulkhu, U.; Mahmoudi, M.; Maurizi, L.; Salaklang, J.; Hofmann, H., Protein corona composition of superparamagnetic iron oxide nanoparticles with various physico-chemical properties and coatings. *Scientific reports* **2014,** *4* (1), 1-9.
45. Tenzer, S.; Docter, D.; Kuharev, J.; Musyanovych, A.; Fetz, V.; Hecht, R.; Schlenk, F.; Fischer, D.; Kiouptsi, K.; Reinhardt, C., Rapid formation of plasma protein corona critically affects nanoparticle pathophysiology. *Nature nanotechnology* **2013,** *8* (10), 772-781.
46. Giulimondi, F.; Vulpis, E.; Digiacomo, L.; Giuli, M. V.; Mancusi, A.; Capriotti, A. L.; Laganà, A.; Cerrato, A.; Zenezini Chiozzi, R.; Nicoletti, C., Opsonin-deficient nucleoproteic corona endows unPEGylated liposomes with stealth properties *in vivo*. *ACS nano* **2022,** *16* (2), 2088-2100.
47. Papini, E.; Tavano, R.; Mancin, F., Opsonins and dysopsonins of nanoparticles: facts, concepts, and methodological guidelines. *Frontiers in immunology* **2020,** *11*, 567365.
48. Li, H.; Wang, Y.; Tang, Q.; Yin, D.; Tang, C.; He, E.; Zou, L.; Peng, Q., The protein corona and its effects on nanoparticle-based drug delivery systems. *Acta Biomaterialia* **2021,** *129*, 57-72.
49. Icer, M. A.; Gezmen-Karadag, M., The multiple functions and mechanisms of osteopontin. *Clinical biochemistry* **2018,** *59*, 17-24.
50. Eigenbrot, C., Structure, function, and activation of coagulation factor VII. *Current protein & peptide science* **2002,** *3* (3), 287-99.
51. Bjørklund, G.; Svanberg, E.; Dadar, M.; Card, D. J.; Chirumbolo, S.; Harrington, D. J.; Aaseth, J., The Role of Matrix Gla Protein (MGP) in Vascular Calcification. *Current medicinal chemistry* **2020,** *27* (10), 1647-1660.
52. Zhao, K. W.; Murray, S. S.; Murray, E. J., Secreted phosphoprotein-24 kDa (Spp24) attenuates BMP-2-stimulated Smad 1/5 phosphorylation and alkaline phosphatase induction and was purified in

a protective complex with alpha2 -Macroglobulins From Serum. *Journal of cellular biochemistry* **2013,** *114* (2), 378-87.
53. Fuior, E. V.; Gafencu, A. V., Apolipoprotein C1: Its Pleiotropic Effects in Lipid Metabolism and Beyond. *International journal of molecular sciences* **2019,** *20* (23).
54. Mathews, S. T.; Chellam, N.; Srinivas, P. R.; Cintron, V. J.; Leon, M. A.; Goustin, A. S.; Grunberger, G., Alpha2-HSG, a specific inhibitor of insulin receptor autophosphorylation, interacts with the insulin receptor. *Molecular and cellular endocrinology* **2000,** *164* (1-2), 87-98.
55. Coates, T. D., Physiology and pathophysiology of iron in hemoglobin-associated diseases. *Free radical biology & medicine* **2014,** *72*, 23-40.
56. Thiele, L.; Diederichs, J. E.; Reszka, R.; Merkle, H. P.; Walter, E., Competitive adsorption of serum proteins at microparticles affects phagocytosis by dendritic cells. *Biomaterials* **2003,** *24* (8), 1409-1418.
57. Mirshafiee, V.; Kim, R.; Park, S.; Mahmoudi, M.; Kraft, M. L., Impact of protein pre-coating on the protein corona composition and nanoparticle cellular uptake. *Biomaterials* **2016,** *75*, 295-304.
58. Tonigold, M.; Simon, J.; Estupiñán, D.; Kokkinopoulou, M.; Reinholz, J.; Kintzel, U.; Kaltbeitzel, A.; Renz, P.; Domogalla, M. P.; Steinbrink, K.; Lieberwirth, I.; Crespy, D.; Landfester, K.; Mailänder, V., Pre-adsorption of antibodies enables targeting of nanocarriers despite a biomolecular corona. *Nat Nanotechnol* **2018,** *13* (9), 862-869.
59. Simon, J.; Müller, L. K.; Kokkinopoulou, M.; Lieberwirth, I.; Morsbach, S.; Landfester, K.; Mailänder, V., Exploiting the biomolecular corona: pre-coating of nanoparticles enables controlled cellular interactions. *Nanoscale* **2018,** *10* (22), 10731-10739.
60. Safavi-Sohi, R.; Maghari, S.; Raoufi, M.; Jalali, S. A.; Hajipour, M. J.; Ghassempour, A.; Mahmoudi, M., Bypassing Protein Corona Issue on Active Targeting: Zwitterionic Coatings Dictate Specific Interactions of Targeting Moieties and Cell Receptors. *ACS applied materials & interfaces* **2016,** *8* (35), 22808-18.
61. Vincent, M. P.; Bobbala, S.; Karabin, N. B.; Frey, M.; Liu, Y.; Navidzadeh, J. O.; Stack, T.; Scott, E. A., Surface chemistry-mediated modulation of adsorbed albumin folding state specifies nanocarrier clearance by distinct macrophage subsets. *Nat Commun* **2021,** *12* (1), 648.
62. Seneca, S.; Simon, J.; Weber, C.; Ghazaryan, A.; Ethirajan, A.; Mailaender, V.; Morsbach, S.; Landfester, K., How Low Can You Go? Low Densities of Poly(ethylene glycol) Surfactants Attract Stealth Proteins. *Macromolecular bioscience* **2018,** *18* (9), e1800075.
63. Müller, J.; Bauer, K. N.; Prozeller, D.; Simon, J.; Mailänder, V.; Wurm, F. R.; Winzen, S.; Landfester, K., Coating nanoparticles with tunable surfactants facilitates control over the protein corona. *Biomaterials* **2017,** *115*, 1-8.
64. Mohammad-Beigi, H.; Hayashi, Y.; Zeuthen, C. M.; Eskandari, H.; Scavenius, C.; Juul-Madsen, K.; Vorup-Jensen, T.; Enghild, J. J.; Sutherland, D. S., Mapping and identification of soft corona proteins at nanoparticles and their impact on cellular association. *Nature Communications* **2020,** *11* (1), 4535.
65. Baimanov, D.; Wang, J.; Zhang, J.; Liu, K.; Cong, Y.; Shi, X.; Zhang, X.; Li, Y.; Li, X.; Qiao, R., In situ analysis of nanoparticle soft corona and dynamic evolution. *Nature Communications* **2022,** *13* (1), 5389.
66. Casals, E.; Pfaller, T.; Duschl, A.; Oostingh, G. J.; Puntes, V. F., Hardening of the nanoparticle–protein corona in metal (Au, Ag) and oxide (Fe3O4, CoO, and CeO2) nanoparticles. *Small* **2011,** *7* (24), 3479-3486.
67. Miclăuş, T.; Bochenkov, V. E.; Ogaki, R.; Howard, K. A.; Sutherland, D. S., Spatial mapping and quantification of soft and hard protein coronas at silver nanocubes. *Nano letters* **2014,** *14* (4), 2086-2093.
68. Deng, Z. J.; Liang, M.; Monteiro, M.; Toth, I.; Minchin, R. F., Nanoparticle-induced unfolding of fibrinogen promotes Mac-1 receptor activation and inflammation. *Nature nanotechnology* **2011,** *6* (1), 39-44.

69. Raoufi, M.; Hajipour, M. J.; Shahri, S. M. K.; Schoen, I.; Linn, U.; Mahmoudi, M., Probing fibronectin conformation on a protein corona layer around nanoparticles. *Nanoscale* **2018,** *10* (3), 1228-1233.
70. Ashkarran, A. A.; Dararatana, N.; Crespy, D.; Caracciolo, G.; Mahmoudi, M., Mapping the heterogeneity of protein corona by *ex vivo* magnetic levitation. *Nanoscale* **2020,** *12* (4), 2374-2383.
71. Sallem, F.; Haji, R.; Vervandier-Fasseur, D.; Nury, T.; Maurizi, L.; Boudon, J.; Lizard, G.; Millot, N., Elaboration of trans-resveratrol derivative-loaded superparamagnetic iron oxide nanoparticles for glioma treatment. *Nanomaterials* **2019,** *9* (2), 287.
72. Sruthi, S.; Maurizi, L.; Nury, T.; Sallem, F.; Boudon, J.; Riedinger, J. M.; Millot, N.; Bouyer, F.; Lizard, G., Cellular interactions of functionalized superparamagnetic iron oxide nanoparticles on oligodendrocytes without detrimental side effects: Cell death induction, oxidative stress and inflammation. *Colloids Surf B Biointerfaces* **2018,** *170*, 454-462.
73. Maurizi, L.; Sakulkhu, U.; Gramoun, A.; Vallee, J.-P.; Hofmann, H., A fast and reproducible method to quantify magnetic nanoparticle biodistribution. *Analyst* **2014,** *139* (5), 1184-1191.
74. Galmarini, S.; Hanusch, U.; Giraud, M.; Cayla, N.; Chiappe, D.; von Moos, N.; Hofmann, H.; Maurizi, L., Beyond unpredictability: the importance of reproducibility in understanding the protein corona of nanoparticles. *Bioconjugate Chemistry* **2018,** *29* (10), 3385-3393.